RI 9645 REPORT OF INVESTIGATIONS/1998

Investigation of Coal Properties and Airborne Respirable Dust Generation

U.S. DEPARTMENT OF HEALTH AND HUMAN SERVICES
Public Health Service
Centers for Disease Control and Prevention
National Institute for Occupational Safety and Health

Report of Investigations 9645

Investigation of Coal Properties and Airborne Respirable Dust Generation

John A. Organiscak and Steven J. Page

U.S. DEPARTMENT OF HEALTH AND HUMAN SERVICES
Public Health Service
Centers for Disease Control and Prevention
National Institute for Occupational Safety and Health
Pittsburgh Research Laboratory
Pittsburgh, PA

October 1998

International Standard Serial Number
ISSN 1066-5552

CONTENTS

ILLUSTRATIONS

TABLES

UNIT OF MEASURE ABBREVIATIONS USED IN THIS REPORT

A	ampere	m^3/s	cubic meter per second
hr	hour	mg/kg	milligram per kilogram
kg	kilogram	mg/m^3	milligram per cubic meter
kg/hr	kilogram per hour	rpm	revolution per minute
kW	kilowatt	s	second
L/min	liter per minute	V	volt
m	meter	V/cm	volt per centimeter
min	minute	W·min	watt minute
mm	millimeter	W·min/kg	watt minute per kilogram
m/s	meter per second	μm	micrometer
m^3/min	cubic meter per minute	%	percent

INVESTIGATION OF COAL PROPERTIES AND AIRBORNE RESPIRABLE DUST GENERATION

By John A. Organiscak[1] and Steven J. Page[2]

ABSTRACT

Laboratory crushing experiments were conducted on a range of low- to high-volatile bituminous coals to investigate the various factors influencing airborne respirable dust (ARD) generation. This research was conducted to identify the principles of ARD liberation from the coal product. Five U.S. bituminous coals were uniformly prepared and processed through a double roll crusher located in a low-velocity wind tunnel. Experimental factors studied included inherent coal seam constituents, coal grindability, specific energy of crushing, product size characteristics, dust cloud electrostatic field, and specific ARD generated.

The results of this investigation indicate that a combination of several factors are associated with ARD generation. One factor is the effect of coal rank, described by the inherent moist fuel ratio, on the product size characteristics, defined by Schuhmann size function parameters. Another key factor is the effect of air dry loss (ADL) moisture in the coal seam on the breakage-induced electrostatic field of airborne dust. The effect of these factors is that different percentages of <10-μm coal particles are dispersed as ARD. A discussion of electrostatic field principles, coal ADL, and its effect on ARD generation is presented.

---

[1]Mining engineer.
[2]Physicist.
Pittsburgh Research Laboratory, National Institute for Occupational Safety and Health, Pittsburgh, PA.

INTRODUCTION

Prolonged exposure to airborne respirable coal dust is responsible for the prevalence of coal workers' pneumoconiosis (CWP) in the United States. Health research studies have identified that the severity of CWP is directly related to the amount of respirable dust exposure and the coal rank [Attfield and Seixas 1995; Attfield and Morring 1992; Hurley and Maclaren 1987]. Since enactment of the 2.0 mg/m^3 dust standard in the Federal Coal Mine Health and Safety Act of 1969 (Public Law 91-173), average dust levels for a continuous mining machine operator were reduced from over 6 mg/m^3 to current levels just under the 2.0 mg/m^3 standard [Attfield and Wagner 1992]. The National Institute for Occupational Safety and Health (NIOSH) recently determined through its Coal Worker's X-Ray Surveillance Program that coal miners continue to have an elevated risk for CWP under the current 2.0 mg/m^3 dust standard and recommended a 1.0 mg/m^3 dust standard to reduce the prevalence of CWP [NIOSH 1995]. To achieve a further reduction in the CWP risk, coal mine worker dust exposure needs to be notably reduced. Determination of the key factors involved in airborne respirable dust (ARD) generation would likely identify the most influential engineering control strategies needed for improving coal mine dust suppression.

Prior research has identified several relationships between coal rank and dust generation. Laboratory coal comminution studies have shown a significantly consistent positive correlation between coal rank (described by Hardgrove grindability index (HGI), fuel ratio, vitrinite reflectance, or level of organic metamorphism) and the amount of respirable-sized particles found in the product [Srikanth et al. 1995; Moore and Bise 1984; Baafi and Ramani 1979]. These studies show conclusively that either a grinding or crushing process produces more product fines and more respirable sized particles in the product fines for higher rank coals.

Other research studies of airborne dust generation and coal rank have shown different relationships compared to the coal rank and coal product size conclusion. The National Coal Board's Mining Research Establishment in the United Kingdom had initially observed discrepancies in airborne dust generation and the coal product size characteristics with respect to the breakage processes of the coal [Knight 1958; Hamilton and Knight 1957]. Laboratory shatter (drop test) and tumble breakage tests (friability type) were conducted on coals of various ranks mined in the United Kingdom and showed negative correlations between compressive strength and the amount of coal fines produced. Although the higher rank weaker coals (lower compressive strength coals) consistently produced more product fines, airborne dust generation differences were observed between these two breakage processes. A negative airborne dust correlation with coal strength (or positive with coal rank) was observed for the tumble tests; however, no airborne dust correlation was observed for the shatter tests. It was concluded that weaker coals (higher rank coals) had a lower percentage of dust present in the product fines dispersed during the shatter breakage tests and that airborne dust generated is somewhat related to the violence upon which the particular coal breaks.

Underground and laboratory studies conducted by the former U.S. Bureau of Mines (USBM) in the late 1980s and early 1990s showed an opposite correlation to coal rank (low- to high-volatile bituminous coals studied) and airborne dust generation compared to previously established coal rank and fines production relationships. An underground survey of 20 longwalls operating in 16 different bituminous coal seams throughout the United States indicated that high-volatile, low-ash coal seams (lower rank bituminous coals) tended to produce more ARD [Organiscak et al. 1992]. Additional USBM laboratory work on crushing nine bituminous types of 4.8- to 5.7-mm-sized feed coals through a small roll crusher (38.1-mm-diam rolls spaced 3.2 mm apart) indicated that lower rank coals, as described by their inherent moist fuel ratio (MFR = (fixed carbon ÷ volatile matter) ÷ inherent moisture), also produced more airborne dust [Page et al. 1993]. Although the general airborne dust and coal rank relationships were similar for the laboratory and underground studies, differences in the correlation of particular coal parameters, such as ash, were presumed to be an extraneous variable associated with the inherent weakness of the coal's cleat (or joint) structure. Others have postulated that coal fragmentation from cutting usually occurs, in part, along planes of imperfections (cleats or joints) or weaknesses containing mineral matter [Stecklein et al. 1982].

To identify the underlying factors involved in various relationships observed between various bituminous coals, strength, product size characteristics, and ARD, the NIOSH Pittsburgh Research Laboratory (PRL) conducted laboratory crushing experiments on larger coal lumps containing inherent planes of weakness (cleats or joints). This research was conducted to formulate the principles of ARD liberation from the coal product. Experimental factors studied include inherent coal constituents, coal HGI, specific energy of crushing, product size characteristics, dust cloud electrostatic field, and specific ARD generated. This report describes the experimental results of roll crushing five different U.S. bituminous coals and discusses the air dry loss (ADL) and electrostatic charge effect on ARD liberation from the coal product.

EXPERIMENTAL DESIGN

The objectives of this research were to (1) develop a repeatable laboratory testing protocol for generating coal ARD and (2) identify key factors influencing ARD generation, where one of the "factors" is different bituminous coals. The intent of this research was not to conduct experiments with a specialized coal-cutting or breakage apparatus, but to use commercially available equipment to accomplish the research objectives. A double roll crusher was selected to study the primary breakage properties of medium-sized coal lumps (approximately 50 mm), because it has a small size reduction ratio of 1.5 to 5:1 (ratio of average feed size to product size) without a significant amount of regrinding [Cummins and Given 1973]. The five different bituminous coals were roll-crushed under uniform procedures to investigate the effects of coal MFR, physical coal strength properties (coal HGI and specific energy of crushing), coal breakage characteristics (product size distribution), and dust cloud electrostatic field on specific ARD generation.

TEST FACILITY

The experimental test facility was comprised of a roll crusher located in the intake end of a 1.2-m-high by 0.6-m-wide wood-framed, plastic sheath-enclosed wind tunnel 6.1 m long. A dust collector and exhaust fan were located at the discharge end of the tunnel. The crusher was a 1.1-kW compact double roll crusher (79.4-mm-diam rolls) operating at approximately 70 rpm with twenty-four 12.7-mm-high staggered teeth on each roll. An inductive current transformer (±0.1 A) was installed to monitor the crusher's current usage. The crusher's operating capacity was 227-1,361 kg/hr of up to 101.6 mm feed-size lumps of coal or rock material.

Dust sampling was conducted 3 m downstream of the crusher and approximately 2.4 m upstream of the tunnel transition to the dust collector and exhaust fan. Dust sampling was conducted with two Sierra 298 personal sampling impactors at 2.0 L/min, each equipped with the standard inlet cowl and positioned at one-half the tunnel height from the floor and one-third the tunnel width from a wall. The impactor stages 1 through 6 (20-μm through 1.55-μm cut point sizes) were used with the <1.55-μm particle sizes collected on the final filter. An MIE RAM-1 sampler continuously monitored the respirable fraction of dust from a 10-mm Dorr-Oliver cyclone located in the middle of the sampling location [Williams and Timko 1984]. All of the sampler inlets were faced into the airflow. Dust cloud electrostatic field measurements were taken immediately downstream of the crusher (within 0.3 m) with a Monroe 245 electrostatic field meter and stored on an analog datalogger. Air velocities were determined from the time it took the dust to travel 3 m to the RAM-1 sampling location after crusher startup. Preliminary crushing tests indicated that the lowest possible wind tunnel air velocity to maximize dust concentrations and mass collection was 0.10 m/s (4.5 m^3/min air quantity). Lower velocities permitted dust to escape from the tunnel inlet; therefore, wind tunnel airflow was targeted for 0.10 m/s for all of the experiments.

EXPERIMENTAL PROCEDURE

The key elements for reducing crushing experimental error are feed size and feed methods. In development of a reproducible crushing procedure, both size and feed methods were studied in a series of crushing experiments conducted on 470 kg of Pittsburgh coal obtained from PRL's Safety Research Coal Mine. A large batch of PRL coal lumps were jaw-crushed, screened, and riffled (a sample splitting process) [Taggart 1945] into 32 representative test samples (14.7 kg by weight) of various feed sizes that would be tested under different feed methods. The sizes to be tested included 50.0 by 25.0 mm, 25.0 by 19.0 mm, 19.0 by 12.5 mm, and an equivalent weight three-size mixture. The two feed methods studied were batch-feed (crusher self-feeds the batch of coal from its hopper approximately 30 s per sample) and trickle-feed (a separate vibrating feeder slowly trickles coal into the crusher, approximately 2 min per sample). The various sized test samples were randomly processed through the crusher for the two feed methods, yielding four runs for each test condition.

The crushing variables studied during these tests included energy consumption, ARD, dust cloud electrostatic field, and Schuhmann size function parameters. Their averages and variations (standard error and coefficient of variation (CV)) are shown in table 1. Energy consumption was determined from crusher current, voltage, and time. ARD was determined by applying the American Conference of Governmental Industrial Hygienists definition of respirable dust to the mass sizes collected on the Sierra 298 impactors, sampling rate, and time [Potts et al. 1990]. The electrostatic field was determined by averaging the field over a time period equal to the crusher operating time plus 10 s. This would allow sufficient time for the generated dust cloud to travel beyond the field meter position. The crusher product was screened for size classification. Schuhmann size function parameters [Schuhmann 1940] defined in table 1 were determined by nonlinear least squares regression of the cumulative size distribution data.

The experimental results shown in table 1 indicate that the batch-feed method for both the size mix and the 50.0- by 25.0-mm feed samples had the lowest amount of measurement error for all of the crusher variables investigated. ARD had the highest variability out of all of the measured variables, but had CVs below 20% for the batch-feed method of the size mix and the 50.0- by 25.0-mm samples. Energy consumption measurements were the least variable for the batch-feed method. The larger variations in energy consumption measurements for the trickle-feed method were likely due to poor resolution of the very low crushing currents measured. Both the electrostatic

Table 1.—Precision of experimental procedures with PRL coal

Feed method and size	Energy consumption, W·min: Mean (ΣX/n)	Energy consumption, W·min: Standard error (s/√n)	Energy consumption, W·min: CV (s/mean)	ARD, mg/m^3: Mean (ΣX/n)	ARD, mg/m^3: Standard error (s/√n)	ARD, mg/m^3: CV (s/mean)	Electrostatic field, V/cm: Mean (ΣX/n)	Electrostatic field, V/cm: Standard error (s/√n)	Electrostatic field, V/cm: CV (s/mean)	Schuhmann size function (all R^2's>0.99): Top size "a", mm	Schuhmann size function: s_a, mm	Schuhmann size function: Exponent "b"	Schuhmann size function: s_b
Batch:													
Mix	77.09	1.91	0.05	6.17	0.57	0.18	119.35	8.45	0.07	15.07	0.11	0.88	0.01
50.0 by 25.0 mm . .	88.00	5.82	0.13	7.38	0.63	0.17	134.55	6.25	0.05	13.78	0.12	0.89	0.01
25.0 by 19.0 mm . .	94.06	0.80	0.02	5.67	1.23	0.43	112.90	7.87	0.07	14.53	0.15	0.86	0.01
19.0 by 12.5 mm . .	66.59	4.11	0.12	5.71	1.29	0.45	115.50	16.50	0.14	17.68	0.15	0.89	0.01
Trickle:													
Mix	35.15	2.38	0.14	4.55	0.79	0.35	118.90	5.69	0.05	15.17	0.17	1.28	0.03
50.0 by 25.0 mm . .	70.73	7.47	0.21	4.53	0.87	0.38	115.15	10.04	0.09	14.31	0.13	1.12	0.02
25.0 by 19.0 mm . .	23.90	7.48	0.63	4.65	0.93	0.40	114.00	9.17	0.08	14.75	0.15	1.31	0.03
19.0 by 12.5 mm . .	22.36	6.12	0.55	3.60	0.77	0.43	77.80	6.38	0.08	16.26	0.18	1.60	0.04

X = variable
n = number of measurements
s = standard deviation
CV = coefficient of variation

Schuhmann size function: $Y = (X/a)^b$,
where Y = cumulative percent of weight less than X,
X = size of particles, mm,
a = Schuhmann top size regression parameter,
b = Schuhmann exponent regression parameter,
s_a = standard error of regression parameter "a",
and s_b = standard error of regression parameter "b".

field measurements and Schuhmann size function parameters had low measurement errors for all of the feed method and size tests. One-half of the test samples were analyzed for coal constituents ([ASTM (1996a)], not shown in table 1) and indicated that CVs for the inherent moisture, ash, volatile, and fixed carbon were all below 10%. These results indicate that representative feed samples were obtained with the feed preparation procedures.

The batch-feed crushing method of a coal size mix was the procedure chosen for minimizing the variable measurement error of the remaining coal ARD generation experiments. The Schuhmann exponent parameters <1 for the batch-feed method indicate that some regrinding occurs compared with the Schuhmann exponent parameters >1 for the trickle-feed method. This parallels the <1 Schuhmann exponent parameters observed with run-of-mine (ROM) coals [Ramani et al. 1987]. The size mix feed was preferred to the 50.0- by 25.0-mm feed because, as bulk coal samples are processed (crushed and screened) to make the feed samples, more feed material can be obtained from a given amount of bulk coal.

SAMPLE COLLECTION

Three bituminous coals were targeted for sample collection. These ranged from a low-volatile, high-ash coal (higher rank) to a high-volatile, low-ash coal (lower rank) with one coal type in the middle of this range. The bulk coal samples were collected at three continuous miner sections located in the Eagle and Upper Freeport Seams in West Virginia and the Blind Canyon Seam in Utah. Three days of coal collection and airborne dust sampling were conducted at each mining section. On each day, both coal and dust samples were collected for one mining cut. The coal was channeled from the entry rib, outby the mined cut. This coal was hand screened and packaged into three sizes of lumps: >50.0-mm, 50.0 by 25.0 mm, and 25.0 by 19.0 mm. Approximately 50 kg of bulk coal was collected each day. ROM product samples were also collected from shuttle cars during the cut at the feeder breaker dump point for size analysis.

Underground dust sampling was conducted in the intake and return of the mined cut. Airborne dust was measured with personal respirable dust samplers, Sierra 298 personal impactors, and a RAM-1 (only at the return location). The operational parameters and dust concentrations measured at the mines visited are shown in table 2, and the airborne dust size characteristics in the mining return air course are shown in figure 1. The airborne dust size distribution data suggest that flooded-bed scrubber (irrigated-filter dust collector) use on the continuous mining machine affected the airborne dust measurements. Airborne dust size data obtained in the Eagle Seam while using a machine-mounted flooded-bed scrubber indicated a noticeably smaller dust size distribution (mean mass aerodynamic diameter (MMAD) = 7.5 μm, geometric standard deviation (GSD) = 3.7) in the return air compared with that at the other two operations (MMAD = 16.2 and 27.8 μm, GSD = 4.2 and 4.3). The continuous miner operation in the Eagle Seam also had a noticeably less face air quantity of 2.9 m^3/s than that at the other operations, suggesting that a notable portion of the face ventilation and ARD was effectively captured by the flooded-bed scrubber at this operation. The operation without a flooded-bed scrubber in the Blind Canyon Seam used the highest ventilation quantity of 24.0 m^3/s and had the largest airborne size distribution (MMAD = 27.8 μm, GSD = 4.3). Because flooded-bed scrubbers were used on two of the continuous mining machines sampled, an ARD generation analysis between mining operations would be unreliable. Therefore, all ARD generation conclusions are based on laboratory crushing experiments using a comparable operating procedure.

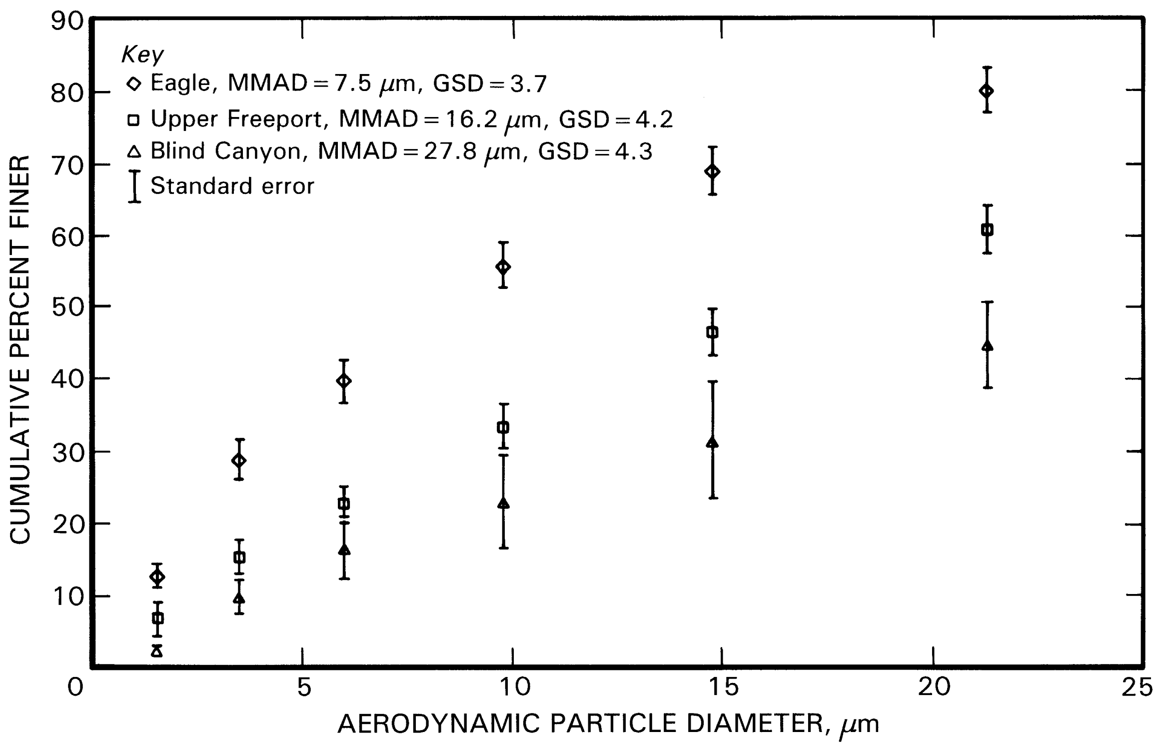

Figure 1.—Airborne dust size distributions measured at underground continuous mining operations.

Table 2.—Underground mine data

Underground parameter	Coal seam: Eagle	Coal seam: Upper Freeport	Coal seam: Blind Canyon
Seam height, m	2.4	2.7	2.7.
Cut depth, m	9.1	7.6	12.2.
Ventilation type	Exhaust curtain	Exhaust tube	Exhaust tube.
Return air quantity, m^3/s[1]	2.89 (0.12)	12.55 (0.47)	24.01 (1.02).
Continuous miner dust controls	Cutter boom sprays, flooded-bed scrubber, radio remote control.	Cutter boom sprays, flooded-bed scrubber, radio remote control.	Cutter boom sprays, spray fan system, radio remote control.
Water added to coal, percent by weight.[2]	3.5 (0.4)	2.5 (0.5)	4.6 (0.3).
[3]Intake respirable dust concentration, mg/m^3.	0.56 (0.10)	1.59 (0.77)	0.40 (0.22).
[3]Return respirable dust concentration, mg/m^3.	2.89 (0.12)	2.94 (0.37)	4.04 (1.01).

NOTE: All measurements for air quantity and dust concentration are averages, followed by standard error in parentheses.
[1]Measurement taken at the return dust sampling location.
[2]Moisture determined from air drying ROM coal samples.
[3]Personal dust sampling at 2 L/min.

The underground bulk coal samples were processed in the laboratory to obtain two mixed size test samples for each mining cut, for a total of six test samples for each mine. Jaw crushing was conducted on the larger lumps to obtain equal portions of feed sizes needed for testing. Riffling was done to split the coal samples from each cut into equal portions. All of the coal test samples were weighed and stored in sealed cans. A high-volatile, high-ash bulk coal, collected from the Wadge Seam in Colorado for another project, was also processed in the same manner to obtain four additional test samples for the crushing experiments. The ROM samples collected from the three mining operations surveyed were also screened for size analysis.

The underground ROM product size distributions confirmed that some coal product regrinding occurs during underground coal cutting. The ROM coal product size distributions are shown in figure 2 and are described by Schuhmann exponent parameters <1. This is similar to the PRL coal product size distribution for the batch-feed crushing procedure.

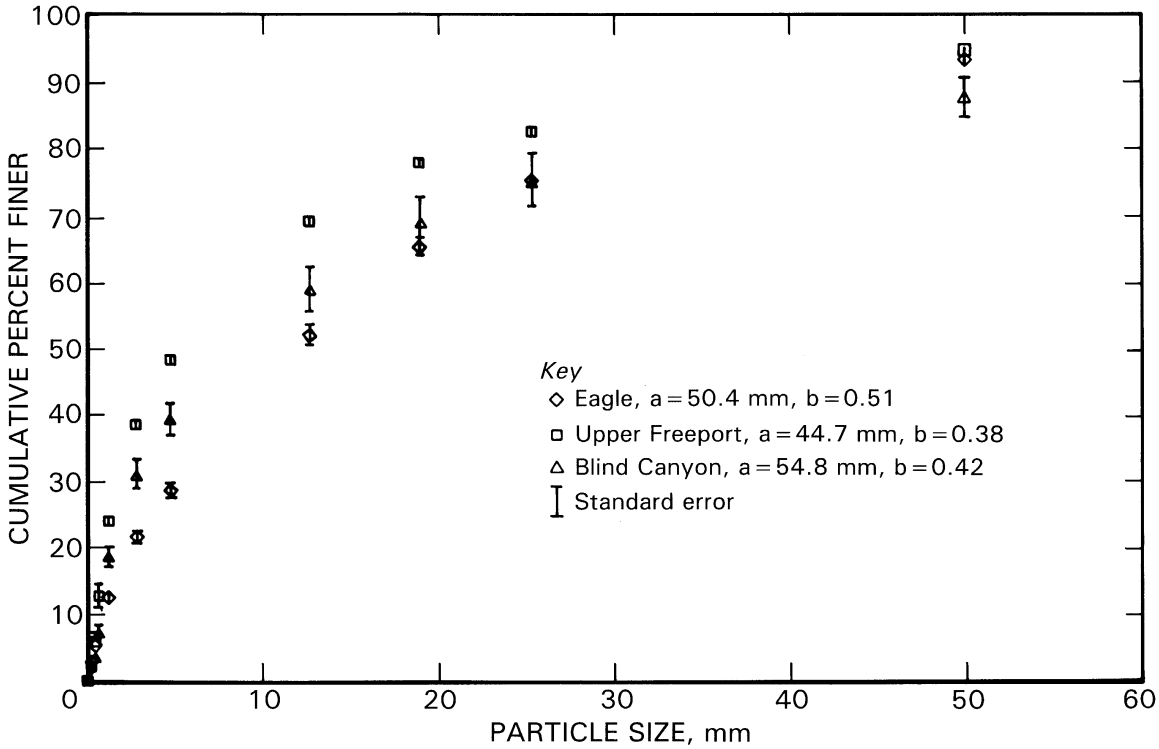

Figure 2.—ROM coal product size distributions from underground continuous mining operations.

EXPERIMENTAL RESULTS

The coal samples were randomly run in the roll crusher test facility using the batch feed of size mix procedure. Experimental factors studied included inherent coal constituents, coal HGI, specific energy of crushing, product size attributes, dust cloud electrostatic field, and specific ARD generated. A small coal test sample was riffled from the crushed product after screening to determine the coal constituents by proximate analysis [ASTM 1996a] and to determine the HGI [ASTM 1996b]. The coal constituent and HGI data are included in table A-1 in the appendix. The specific energy is the energy consumed per unit weight of the coal sample crushed. The specific ARD is the total amount of ARD generated in the airstream per unit of material crushed. The four batch-feed, size-mix tests run on PRL's Pittsburgh coal were also included in this data analysis. Thus, 26 tests were completed by the same crushing procedure on five low- to high-volatile bituminous coals. All of the experimental data are included in table A-2 in the appendix.

Good experimental precision was obtained for each seam tested. The average coal constituents (with standard errors) for the five bituminous coal seams tested are shown in table 3. Low sample variability for each coal seam tested was achieved with the coal collection and sample preparation procedures. Figures 3 and 4 show the average coal product and airborne dust size distributions (with standard error bars) for each of the coal seams tested. The coal size distributions illustrate that the various bituminous coals have distinct breakage attributes when crushed under a uniform process. The airborne dust size distributions generated for the various coal seams were more consistent than the coal product size distributions.

DATA ANALYSIS PROCEDURES

Associations between the experimental variables measured were primarily analyzed by both parametric correlations and scatter plot examination. The linear correlations, sample size, and significance levels between inherent coal constituents, coal HGI, specific energy of crushing, Schuhmann size function parameters, dust cloud electrostatic field, and specific ARD generated are shown in table 4. Multivariate statistical description of ARD with the variables measured was hindered by the interdependence of many of the inherent coal constituents and size parameter variables and by the limited number of data points.

The strongest linear and nonlinear associations of importance are shown in figures 5 through 8. Specific energy, Schuhmann size function parameters, amount of dust present in the coal product, dust cloud electrostatic field, and specific ARD are presented with respect to coal rank, as described by its MFR, in figures 5-6. Specific ARD and dust cloud electrostatic field are presented with respect to ADL moisture in the coal in figure 7. Specific ARD generation is expressed as a normalized variable for the specific amount of <10-μm dust particles in the coal product (percentage of respirable dust that becomes airborne) and presented with respect to ADL and electrostatic field measurements in figure 8.

Table 3.—Constituents of coal seams used in roll crusher experiments

Coal seam	ADL[1]	Inherent moisture[2]	Ash content[2]	Volatile matter[2]	Fixed carbon[2]
Eagle	1.0 (0.0)	0.5 (0.0)	7.2 (0.6)	32.2 (0.2)	60.1 (0.5)
Upper Freeport	1.1 (0.0)	0.3 (0.0)	18.5 (0.8)	16.6 (0.1)	64.7 (0.8)
Blind Canyon	3.2 (0.2)	1.4 (0.2)	6.7 (0.8)	43.6 (0.2)	48.2 (0.7)
Wadge	5.2 (0.2)	2.9 (0.3)	12.9 (0.7)	38.3 (0.4)	45.8 (0.2)
Pittsburgh (PRL) . . .	0.9 (0.1)	0.9 (0.1)	6.0 (0.3)	37.3 (0.2)	55.8 (0.0)

NOTE: All measurements are averages, followed by standard error in parentheses.
[1]Reported as percent-weight on an as-received basis.
[2]Reported as percent-weight on an as-determined basis (weight percentages determined without the ADL).

Table 4.—Linear correlations of coal constituents and experimental variables

Parameter	Coal HGI	Specific energy of roll crusher	Schumann top size "a"[1]	Schuhmann exponent "b"[1]	Electrostatic field	Specific ARD
ADL:[2]						
Correlation coefficient . . .	−0.650	−0.102	0.739	0.759	−0.843	0.155
Sample size	24	26	26	26	26	26
Significance level	0.001	0.620	0.000	0.000	0.000	0.451
Inherent moisture:[3]						
Correlation coefficient . . .	−0.685	0.027	0.737	0.869	−0.801	−0.040
Sample size	24	26	26	26	26	26
Significance level	0.000	0.896	0.000	0.000	0.000	0.847
Ash content:[3]						
Correlation coefficient . . .	0.726	−0.770	−0.549	−0.392	0.214	−0.182
Sample size	24	26	26	26	26	26
Significance level	0.000	0.000	0.004	0.047	0.293	0.372
Volatile matter:[3]						
Correlation coefficient . . .	−0.956	0.666	0.907	0.750	−0.611	0.250
Sample size	24	26	26	26	26	26
Significance level	0.000	0.000	0.000	0.000	0.001	0.219
Fixed carbon:[3]						
Correlation coefficient . . .	0.871	−0.353	−0.932	−0.847	0.778	−0.206
Sample size	24	26	26	26	26	26
Significance level	0.000	0.077	0.000	0.000	0.000	0.312
Fuel ratio:[4]						
Correlation coefficient . . .	0.988	−0.679	−0.902	−0.820	0.672	−0.175
Sample size	24	26	26	26	26	26
Significance level	0.000	0.000	0.000	0.000	0.000	0.392
Inherent moist fuel ratio (MFR):[5]						
Correlation coefficient . . .	0.986	−0.681	−0.881	−0.834	0.674	−0.134
Sample size	24	26	26	26	26	26
Significance level	0.000	0.000	0.000	0.000	0.000	0.514
Specific energy of roll crusher:						
Correlation coefficient . . .	−0.647	1.000	0.423	0.360	−0.188	−0.069
Sample size	24	26	26	26	26	26
Significance level	0.001	0.000	0.032	0.071	0.358	0.738
Schuhmann top size "a":[1]						
Correlation coefficient	−0.935	0.423	1.000	0.803	−0.752	0.370
Sample size	24	26	26	26	26	26
Significance level	0.000	0.031	0.000	0.000	0.000	0.063
Schuhmann exponent "b":[1]						
Correlation coefficient	−0.882	0.360	0.803	1.000	−0.866	−0.122
Sample size	24	26	26	26	26	26
Significance level	0.000	0.071	0.000	0.000	0.000	0.554

[1]Schuhmann size function Y = (X/a)b.
[2]Reported as percent-weight on an as-received basis.
[3]Reported as percent-weight on an as-determined basis (weight percentages determined without the ADL).
[4]Fuel ratio is defined as fixed carbon ÷ volatile matter.
[5]Inherent moist fuel ratio is defined as fuel ratio ÷ inherent moisture.

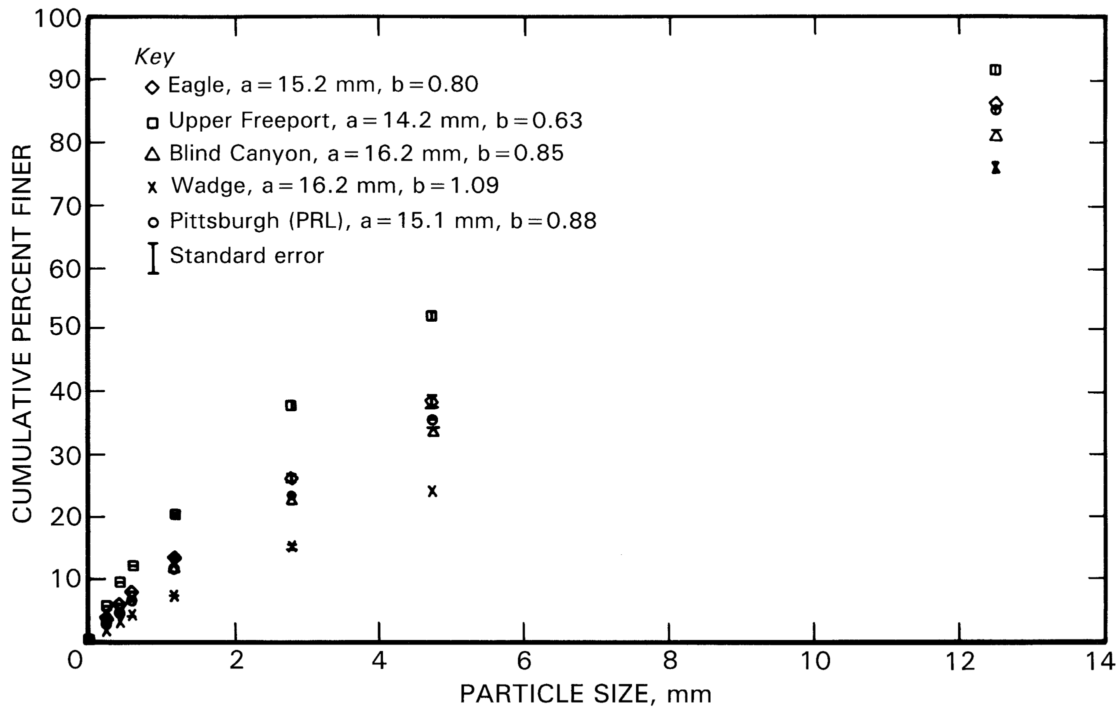

Figure 3.—Roll crusher coal product size distributions.

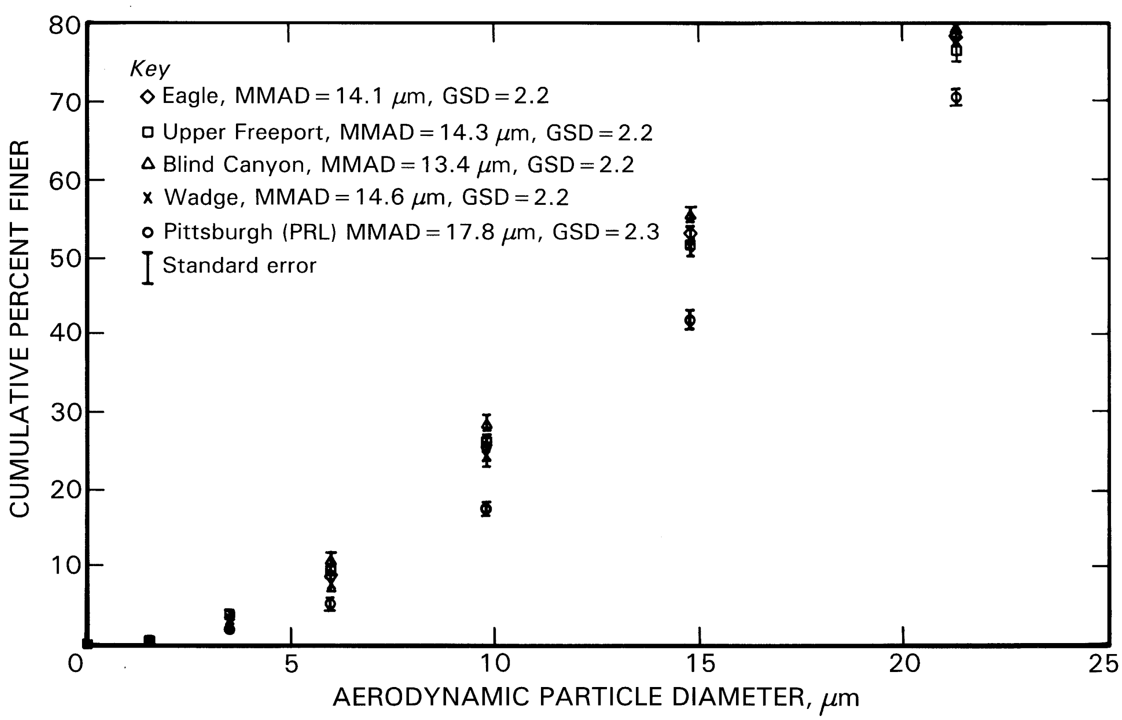

Figure 4.—Roll crusher airborne dust size distributions.

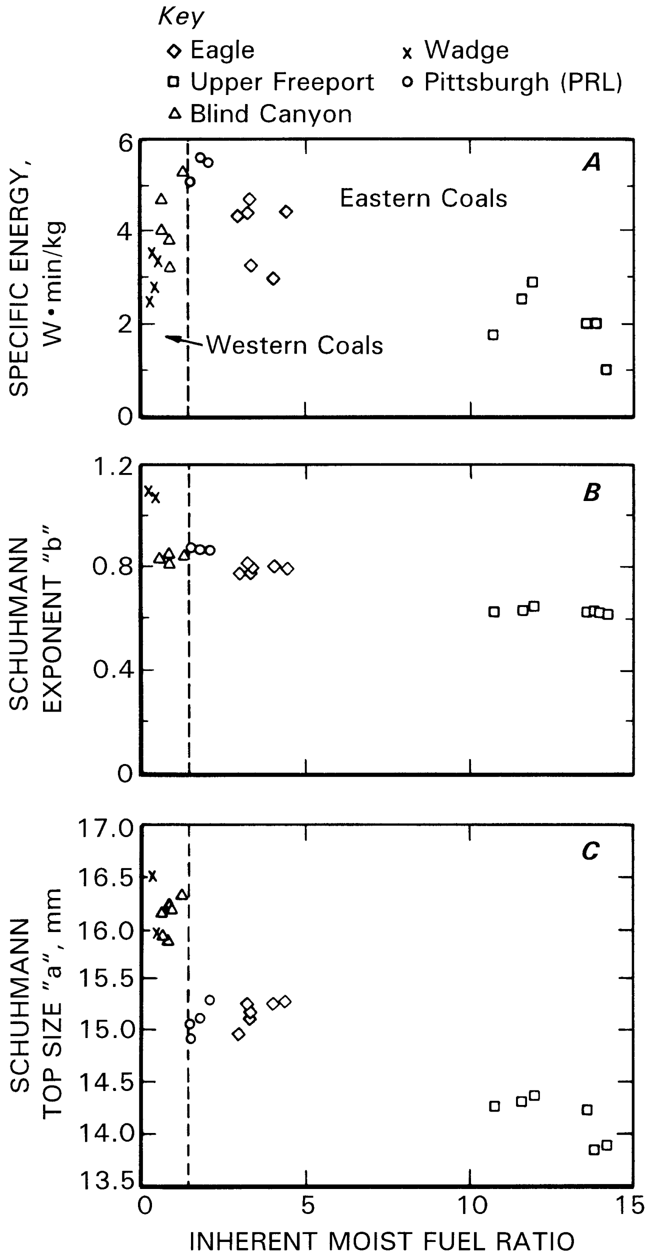

Figure 5.—MFR relationships with energy and Schuhmann size function parameters.

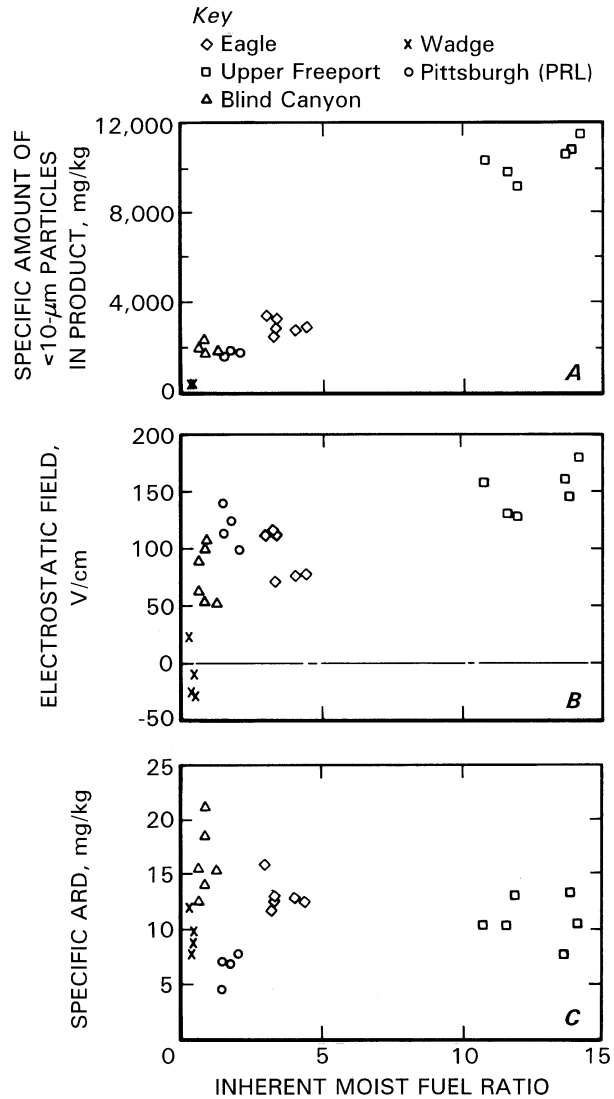

Figure 6.—MFR relationships with product dust fines, electrostatic field, and specific ARD.

PRODUCT SIZE

Results of the roll crushing tests show that the higher MFR coals are significantly correlated with HGI and a smaller product sized distribution. Table 4 shows the linear correlations of inherent coal seam parameters and experimental variables measured. All of the inherent coal constituents are significantly correlated to HGI and Schuhmann size function parameters (significance levels < 0.05). The MFR had one of the highest linear correlations to HGI and Schuhmann size function parameters. Noticeably lower correlations were observed between roll crusher specific energy and many of the coal constituents, MFR, and Schuhmann size function parameters, which suggests that some unquantified factor(s) in this experiment influenced the coal crushing specific energy.

Scatter plot examination of coal constituents, MFR, crusher specific energy, and Schuhmann size function parameters indicate that nonlinear associations exist between some of these variables. One notable nonlinear association is between the coal's MFR and crusher specific energy (see figure 5*A*). Specific energy seems to have a direct relationship for MFRs below 1 (two western U.S. coals tested) and an indirect relationship for MFRs above 1 (three eastern U.S. coals tested). An apparent physical difference that may explain the inconsistent energy relationship between these two coal groups (eastern and western) is that the eastern coals

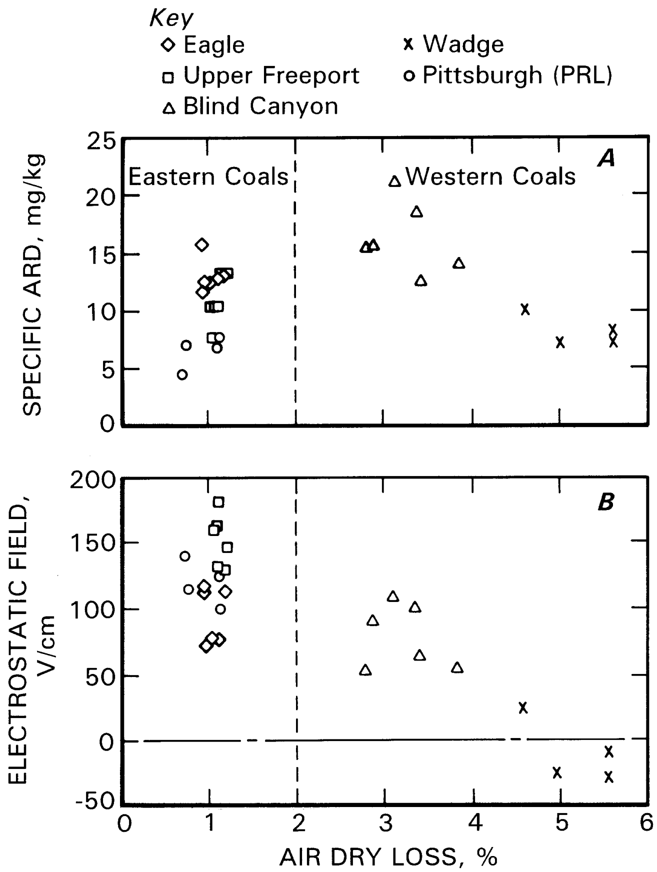

Figure 7.—ADL relationships with specific ARD and electrostatic field.

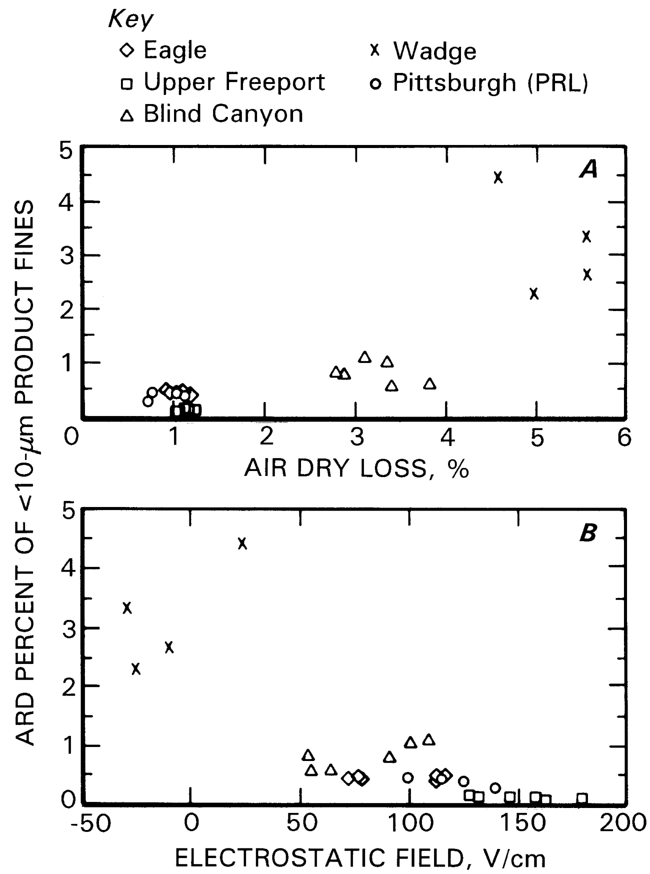

Figure 8.—Normalized ARD percentage dispersed from product with respect to ADL and electrostatic field.

tested tended to have a more distinguishable cleat system than the western coals (eastern coals had more planes of weakness than the western coals).

MFR also has strong relationships between the Schuhmann size function parameters, exhibiting a direct linear relationship to smaller dust particles in the coal product. These breakage attributes can be observed in plots of the coal's MFR and the Schuhmann size function parameters (see figures 5*B* and 5*C*). As the MFR increases, both Schuhmann size function parameters decrease, resulting in a finer coal product size distribution with more fine particles in the coal product. This direct relationship between MFR and respirable-sized dust particles in the coal product (defined as <10 μm) is shown in figure 6*A*. The specific amount of <10-μm dust particles in the product is determined from the Schuhmann size function parameters measured for each test. This analysis assumed that the weight of <10-μm coal particles can be reasonably projected by the Schuhmann size function parameters. All of the Schuhmann size function parameters are efficient (R^2's > 0.99) for size data between 250 μm and 12.5 mm. Others have shown this same direct effect between coal rank and product fines [Srikanth et al. 1995; Moore and Bise 1984; Baafi and Ramani 1979].

ARD GENERATION

The amount of specific ARD generated from roll crushing was not conclusively correlated with any one of the coal constituents, MFR, amount of fines produced, or specific energy, but involved the amount of ADL moisture in the coal and the dust cloud electrostatic field. Table 4 shows dust cloud electrostatic field and specific ARD correlations with coal seam constituents, MFR, crusher specific energy, and Schuhmann size function parameters. The electrostatic field had significant correlations to most of the coal constituents, MFR, and the Schuhmann size function parameters of the crushed coal; the strongest correlations were to the ADL and inherent moisture constituents. Insignificant linear ARD correlations were observed for all of the coal constituents, MFR, Schuhmann size function parameters, and crusher specific energy consumption. Figure 6 shows that, although the MFR is directly related to the amount of <10-μm fines in the product (see figure 6*A*) and the dust cloud electrostatic field (see figure 6*B*), it is not associated with specific ARD generated (see figure 6*C*). Others have observed similar coal rank discrepancies between the amount of fine coal particles produced and the amount of airborne dust generated [Knight 1958; Hamilton and Knight 1957].

Scatter plot analysis of specific ARD data with all of the coal constituents and crushing variables indicates that the best systematic association observed with specific ARD was the amount of ADL moisture in the coals tested (see figure 7*A*). ADL also had the strongest correlation with electrostatic field measurements (see figure 7*B*). ADL moisture is the free water present in the coal's internal fracture structure, with a normal vapor pressure of water [Leonard 1979]. Inherent moisture is bound water in the internal pore structure of the coal, with a vapor pressure lower than normal [Leonard 1979]. Inherent moisture in the coals tested showed a less systematic association with specific ARD, but also had a strong linear correlation to electrostatic field.

The graph of the ADL moisture and specific ARD (figure 7*A*) shows that the correlation is separated into two distinct groups of data: a group below (eastern coals) and above (western coals) 2% ADL moisture. The eastern coals below 2% ADL had considerable variability in specific ARD generated for a very small change in ADL moisture. Western coals had a less sensitive and negative association between specific ARD and ADL moisture.

ADL moisture and dust cloud electrostatic field also have similar data groupings (see figure 7*B*). The electrostatic field measurements for eastern coals are much more variable for a small range in ADL moisture compared with those for the western coals tested. Coal types with <2% ADL moisture (eastern coals) also tended to generate higher electrostatic fields in their airborne dust clouds compared with coals having >2% ADL moisture (western coals). Other researchers, e.g., Polat et al. [1993], have shown that there are almost equal numbers of positively and negatively charged particles for coals, resulting in a net neutral dust cloud. However, these past research results may be indicative of the process of redispersing dust as opposed to producing fresh airborne dust from comminution. The electrostatic fields measured in this study and shown in figure 7*B* suggest that, although some coal types may exhibit close to net neutral fields, the particle charging associated with some eastern coal types has a net positive polarity due to primary breakage.

The above results indicate that no single factor is decisively associated with ARD generation; rather, ARD generation is likely the result of several interrelated factors. These factors involve coal fines production, ADL moisture, and/or dust cloud electrostatic field, all of which are associated with coal MFR. Due to the limited number of tests and the interdependence of these measured variables, statistical model building was prohibitive. To provide some insight into ARD produced, the specific ARD generated was normalized for the specific amount of <10-μm dust particles in the product.

Figure 8 shows the percentage of respirable dust that becomes airborne from the <10-μm product fines compared with ADL moisture and dust cloud electrostatic field, respectively. These graphs indicate that the amount of product fines that become airborne as respirable dust is positively correlated (0.839) with ADL moisture (figure 8*A*) and negatively correlated (−0.802) with electrostatic field (figure 8*B*). This analysis indicates that although higher MFR coals produce more fines, they seem to have a smaller percentage of respirable particles that become airborne because of some effect associated with coal ADL moisture and/or dust cloud electrostatic field. We postulate that the ADL moisture would likely influence the resultant electrostatic charge of the dust fines immediately after coal breakage by providing leakage paths for charge dissipation. The electrostatic field could reflect the strength of dust fines attachment to larger particles before airborne entrainment and/or reflect airborne agglomeration of respirable size particles to larger dust particles.

DISCUSSION

ADL AND CHARGE EFFECT

The data represented in table 4 and in figures 5-7 show complex interactions between the numerous interrelated factors measured. Although distinct trends are observed, there are not sufficient data to formulate a predictive model. However, a descriptive mathematical representation based on established physical laws is suggested. This mathematical representation involves the association observed between specific ARD and ADL. From Figure 7*A*, it is observed that the data, despite the absence of a peak at an ADL of 2%, could follow a set of serpentinelike curves having the functional form

$$y = \frac{abx^{l}}{(a^{m} + x^{m})^{n/2}}$$

$$l = 0,1,2,3$$

$$m = 2,3,4$$

$$n = 1,2,3$$

$$a,b = \text{constants}$$

The special case $l = 1$, $m = 2$, $n = 2$ is the *serpentine function*. Although it was studied and named by Sir Isaac Newton in 1701, the serpentine had been studied earlier by de L'Hôpital and Huygens in 1692. These serpentinelike functions have significant physical importance in that they recur frequently in solutions that describe gravitational and electrostatic fields. Because of the same inverse square law (differing only by constants) of both gravitational and electrostatic fields, these functional forms can be obtained for certain volumetric mass and charge distributions. As an example, the electrostatic field of an electric dipole has the electric field E at points along the perpendicular bisector of the dipole axis (x) given by

$$E = \frac{2aq}{4\pi\epsilon_0(a^2 + x^2)^{3/2}}$$

$$l = 0$$

$$m = 2$$

$$n = 3$$

where ϵ_0 = permittivity of free space,

$2a$ = charge separation,

and q = charge magnitude.

For distances where $x \gg a$, the essential properties of this charge distribution, defined as $2aq = p$, the electric dipole moment, enter only as a product. This means that if E is measured at various distances from the dipole, q and $2a$ can never be deduced separately, but only as the product $2aq$. If q were doubled and a simultaneously halved, E at large distances from the dipole would not change. If the dust clouds generated by the crusher in these tests are considered to consist of particles of positive and negative charge (not necessarily equal in magnitude), then E may be considered to be a vector sum of many electric dipoles having distributions of a and q. The resultant field could have a serpentinelike functional form.

In the presently described tests, E was measured at a fixed point with the generated three-dimensional dust cloud passing over the fixed measuring point. This is the equivalent of measuring E at various points r along the same direction of motion for a fixed dust cloud charge distribution in each test. Assuming varying degrees of charge state for the different coal samples crushed, the variations in E measured might be expected to have a form similar to

$$E \propto \frac{2F(a)G(q)}{4\pi\epsilon_0(F^m(a) + r^m)^{n/2}},$$

where $F(a) = F(a\{\text{MFR}\})$ = some function that represents the dipole charge separations to be dependent on the airborne dust cloud concentration (higher concentrations imply smaller mean particle separation), presumed to be affected by the coal MFR;

and $G(q) = G(q\{\text{ADL}\})$ = some function that represents the dipole charge magnitude, presumed to be affected by the coal ADL.

In a fashion similar to the previously discussed characteristic of p, the same field can be obtained at a different point for variations in q (determined in large part by the ADL) merely by adjusting r. Therefore, a serpentinelike functional relationship can be reasonably expected to exist between the specific ARD generated and the charge-associated variable ADL, as shown in figure 7*A*. However, due to the complexity of the dynamic charge distribution and lack of data about the ADL = 2% value, further investigations of additional coal seams and other parameters that may be significant are required.

DUST CONTROL AND HEALTH IMPACTS

Given that the coal product size characteristics and the percentage of <10-μm dust particles entrained into the air both affect the amount of ARD generated, aspects of these coal properties should be exploitable for ARD control. Previous laboratory research has consistently shown that reducing the amount of energy expended on comminution and/or increasing bit penetration of cutting a given coal will increase the coal product size distribution and reduce the amount of ARD generated [Pomeroy 1963; Kurth et al. 1975; Strebig and Zeller 1975; Roepke et al. 1976]. Several field studies substantiated that changing coal-cutting systems to increase bit penetration reduced ARD [Brooker 1979; Ludlow and Jankowski 1984]. Thus, a key element to dust control is improving the energy efficiency of cutting systems to increase product size and reduce ARD generation.

Another element of dust control involves the suppression and/or capture of ARD. Research has shown that coal wetting reduces ARD generated from breakage; however, the wetting effectiveness varies for coal rank, degrees of mixing, and time after application [Knight 1958]. Past research on water additives (surfactants) to improve coal wettability and ARD suppression has resulted in mixed and inconclusive results [Kost et al. 1981]. A more recent laboratory surfactant study on coal wettability and airborne dust capture from water sprays has shown that a coal powder sink test may be a good initial screening tool for surfactant selection, but does not necessarily predict its airborne dust capture effectiveness [Kim and Tien 1993]. Additional laboratory research on water spray droplet charging with respect to concentration of cationic surfactants showed a strong correlation between water droplet charge and airborne coal dust capture [Polat et al. 1993]. These research findings suggest that coal wettability is not the only key element involved in spray dust suppression effectiveness; electrostatic charge properties of the coal dust cloud and spray droplets may be another influential factor involved in a surfactant's ability to suppress or capture ARD.

One final aspect that the electrostatic charge properties of coal dust observed in this study may have on coal mine worker health is lung dust deposition. Previous research has shown that lung deposition of aerosol particles increases directly with the aerosol's charge properties [Melandri et al. 1983]. Prior coal mine worker health studies have shown an increased prevalence of CWP for higher rank coals [Attfield and Seixas 1995; Attfield and Morring 1992; Hurley and Maclaren 1987]. This coal rank and CWP relationship may be in part related to the increase in dust cloud charging properties of higher rank bituminous coals observed in this research study and the increase in lung deposition observed by Melandri et al. [1983].

CONCLUSIONS

A reproducible laboratory coal-crushing test procedure for ARD generation was developed, and ARD generation was related to multiple factors associated with coal rank. A coal feed mix of equal portions of 50.0- by 25.0-mm, 25.0- by 19.0-mm, and 19.0- by 12.5-mm coal sizes processed through a double roll crusher in a wind tunnel provided the least amount of error in the laboratory measurements. Experimental factors studied were inherent coal constituents, coal HGI, specific energy of crushing, product size attributes, dust cloud electrostatic field, and specific ARD generation. Five low- to high-volatile U.S. bituminous coals were studied using the coal-crushing procedure developed.

Results of these crushing experiments indicate that a combination of several factors are associated with specific ARD generation. MFR was directly correlated with more coal product fines and dust cloud electrostatic field, but did not have the same conclusive correlation with specific ARD. Specific energy had a nonlinear association with MFR and seemed to be noticeably influenced by the coal cleat structure. No significant correlations were observed between specific energy and either dust cloud electrostatic field or specific ARD. The amount of ADL moisture in the coal had the best association with both the dust cloud electrostatic field and the specific ARD generated. Examination of the specific ARD normalized for the specific amount of <10-μm product fines indicates that the net effect of coal MFR, fines production, ADL moisture, and/or electrostatic field properties result in different percentages of product fines becoming ARD. Results from the five coals tested show that the higher MFR bituminous coals had lower percentages of ARD generation per amount of dust fines produced with higher dust cloud electrostatic field values. Future research should focus on determining if coal dust charging properties can be exploited by surfactant application to improve water spray dust suppression and if worker CWP is in part influenced by higher dust-charging properties of higher MFR coals.

REFERENCES

ASTM [1996a]. ASTM D3172—Standard practice for proximate analysis of coal and coke. Annual book of ASTM standards: Vol. 05.05. Philadelphia, PA: American Society for Testing and Materials, pp. 288-297.

ASTM [1996b]. ASTM D409—Standard test method for grindability of coal by the Hardgrove machine method. Annual book of ASTM standards: Vol. 05.05. Philadelphia, PA: American Society for Testing and Materials, pp. 168-175.

Attfield MD, Morring K [1992]. An investigation into the relationship between coal workers' pneumoconiosis and dust exposure in U.S. coal miners. Am Ind Hyg Assoc J *53*(8):486-492.

Attfield MD, Seixas NS [1995]. Prevalence of pneumoconiosis and its relationship to dust exposure in a cohort of U.S. bituminous coal miners and ex-miners. Am J Ind Med *27*:137-151.

Attfield MD, Wagner G [1992]. Respiratory disease in coal miners. In: Rom WN, ed. Environmental and Occupational Medicine. 2nd ed. Boston, MA: Little, Brown and Co., pp. 325-344.

Baafi EY, Ramani RV [1979]. Rank and maceral effects on coal dust. Int J Rock Mech and Min Sci & Geomech Abstr *16*:107-115.

Brooker CM [1979]. Theoretical and practical aspects of cutting and loading by shearer drums—part I. Colliery Guardian Coal Int *227*(1):9-16.

Cummins AB, Given IA [1973]. SME Mining Engineering Handbook: Section 28.3.1-Crushing. New York, NY: Society of Mining, Metallurgy, and Exploration, Inc.: pp. 28-13 to 28-14.

Hamilton RJ, Knight G [1957]. Laboratory experiments on dust suppression with broken coal. London, U.K.: National Coal Board, Mining Research Establishment Report No. 2083, 1957 Research Programme Reference No. 9.2.

Hurley JF, Maclaren WM [1987]. Dust-related risks of radiological changes in coal miners over a 40-year working life: report on work commissioned by NIOSH. Edinburgh, Scotland, U.K.: Institute of Occupational Medicine, Report No. TM/87/09.

Kim J, Tien JC [1993]. Enhanced dust suppression using surfactants. In: Proceedings of the 6th U.S. Mine Ventilation Symposium. Littleton, CO: Society for Mining, Metallurgy, and Exploration, Inc., pp. 523-528.

Knight G [1958]. The formation of dust and debris and the dispersion of dust at the breakage of lump coal in relation to the strength, the water content and superficial wetting. London, U.K.: National Coal Board, Mining Research Establishment Report No. 2088, 1958 Research Programme Reference No. 9.2.

Kost JA, Yingling JC, Mondics BJ [1981]. Guidebook for dust control in underground mining. Bituminous Coal Research, Inc. USBM contract No. J0199046, pp. 65-69.

Kurth DI, Sundae LS, Schultz CW [1975]. Dust generation and comminution of coal. Pittsburgh, PA: U.S. Department of the Interior, Bureau of Mines, RI 8068.

Leonard JW [1979]. Properties of coal and coal impurities. In: Coal preparation. 4th ed. New York, NY: Society for Mining, Metallurgy, and Exploration, Inc., pp. 1-31.

Ludlow J, Jankowski RA [1984]. Use lower shearer drum speeds to achieve deeper coal cutting. Mining Eng *36*(3):251-255.

Melandri C, Tarroni G, Podi V, De Zaiacomo T, Formignani M, Lombardi CC [1983]. Deposition of charged particles in the human airways. J Aerosol Sci *14*(15):657-669.

Moore MP, Bise CJ [1984]. The relationship between the Hardgrove grindability index and the potential for respirable dust generation. In: Proceedings of the Coal Mine Dust Conference, Generic Mineral Technology Center for Respirable Dust. Morgantown, WV: West Virginia University, pp. 250-255.

NIOSH [1995]. Criteria for a recommended standard: occupational exposure to respirable coal mine dust. Cincinnati, OH: U.S. Department of Health and Human Services, Public Health Service, Centers for Disease Control and Prevention, National Institute for Occupational Safety and Health, DHHS (NIOSH) Publication No. 95-106.

Organiscak JA, Page SJ, Jankowski RA [1992]. Relationship of coal seam parameters and airborne respirable dust at longwalls. Pittsburgh, PA: U.S. Department of the Interior, Bureau of Mines, RI 9425.

Page SJ, Organiscak JA, Quattro J [1993]. Coal proximate analyses correlation with airborne respirable dust. Fuel *72*(7):965-970.

Polat H, Hu Q, Polat M, Chander S [1993]. The effect of droplet and particle charge on dust suppression by wetting agents. In: Proceedings of the 6th U.S. Mine Ventilation Symposium. Littleton, CO: Society for Mining, Metallurgy, and Exploration, Inc., pp. 535-541.

Pomeroy CD [1963]. The breakage of coal by wedge action. Colliery Guardian *207*(5354):672-677.

Potts JD, McCawley MA, Jankowski RA [1990]. Thoracic dust exposures on longwall and continuous mining sections. J Appl Occup Environ Hyg *5*(7): 440-447.

Ramani RV, Mutmansky JM, Bhaskar R, Qin J [1987]. Fundamental studies on the relationship between quartz levels in the host material and the respirable dust generated during mining. Vol. I: Experiments, results, and analysis. University Park, PA: PA State Univ. USBM contract No. H0358031.

Roepke WW, Lindroth DP, Myren TA [1976]. Reduction of dust and energy during coal cutting using point-attack bits. With an analysis of rotary cutting and development of a new cutting concept. Pittsburgh, PA: U.S. Department of the Interior, Bureau of Mines, RI 8185.

Schuhmann R [1940]. Principles of comminution, I-size distribution and standard calculations. American Institute of Mining, Metallurgical, and Petroleum Engineers, Inc., TO 1189, Mining Technol *July*:1-11.

Srikanth R, Zhao R, Ramani RV [1995]. Relationships between coal properties and respirable dust generation. In: Proceedings of the 7th U.S. Mine Ventilation Symposium. Littleton, CO: Society for Mining, Metallurgy, and Exploration, Inc., pp. 301-309.

Stecklein GL, Branstetter R, Arrowood R, Davidson D, Lankford J, Lyle R, Nulton C [1982]. Basic research on coal fragmentation and dust entrainment. Vol. I-Technical information. San Antonio, TX: Southwest Research Inst. USBM contract No. J0215009.

Strebig KC, Zeller HW [1975]. The effect of depth of cut and bit type on the generation of respirable dust. Pittsburgh, PA: U.S. Department of the Interior, Bureau of Mines, RI 8042.

Taggart AF [1945]. Handbook of mineral dressing. Section 19—Sampling and testing. New York, NY: John Wiley and Sons, pp. 19-33 to 19-35.

Williams KL, Timko RJ [1984]. Performance evaluation of a real-time aerosol monitor. Pittsburgh, PA: U.S. Department of the Interior, Bureau of Mines, IC 8968.

APPENDIX.—COAL CRUSHING DATA

Table A-1.—Properties of coal samples tested

Coal seam	Sample No.	ADL[1]	Inherent moisture[2]	Ash content[2]	Volatile matter[2]	Fixed carbon[2]	HGI
Eagle	1	1.89	0.57	5.60	32.45	61.38	62
Eagle	2	0.93	0.64	5.41	32.35	61.60	60
Eagle	3	0.97	0.55	8.24	32.39	58.82	55
Eagle	4	0.94	0.58	9.24	31.37	58.81	55
Eagle	5	1.11	0.47	7.25	32.00	60.28	59
Eagle	6	1.03	0.42	7.54	32.47	59.57	58
Upper Freeport	1	1.20	0.29	17.64	16.38	65.69	91
Upper Freeport	2	1.11	0.29	17.32	16.17	66.22	91
Upper Freeport	3	1.10	0.34	16.33	16.94	66.39	89
Upper Freeport	4	1.05	0.37	17.85	16.54	65.24	87
Upper Freeport	5	1.16	0.32	21.26	16.34	62.08	89
Upper Freeport	6	1.08	0.27	20.40	16.96	62.37	89
Blind Canyon	1	3.82	1.42	5.49	43.47	49.62	49
Blind Canyon	2	3.40	1.83	5.31	43.63	49.23	49
Blind Canyon	3	3.10	1.21	10.32	42.54	45.54	48
Blind Canyon	4	2.79	0.83	8.09	44.32	46.76	46
Blind Canyon	5	3.35	1.34	6.02	43.72	48.92	48
Blind Canyon	6	2.87	1.84	5.09	44.03	49.04	47
Wadge	1	4.57	3.75	11.49	38.41	46.35	42
Wadge	2	5.55	2.43	12.22	39.46	45.46	42
Wadge	3	4.96	3.06	13.45	37.54	45.95	43
Wadge	4	5.55	2.50	14.49	37.71	45.30	43
Pittsburgh (PRL) . .	1	0.77	0.98	5.40	37.89	55.73	NA
Pittsburgh (PRL) . .	2	0.74	1.00	5.87	37.48	55.65	NA
Pittsburgh (PRL) . .	3	1.13	0.73	6.66	36.80	55.81	51
Pittsburgh (PRL) . .	4	1.12	0.84	6.15	37.17	55.84	51

NA Data not available.

[1]Reported as percent-weight on an as-received basis.

[2]Reported as percent-weight on an as-determined basis (weight percentages determined without the ADL).

Table A-2.—Experimental data

Coal seam	Sample No.	Feed weight, kg	Crush time, min	Crusher current,[1] A	Air quantity, m^3/min	Schuhmann top size "a", mm	Schuhmann exponent "b"	Electro-static field, V/cm	ARD level,[2] mg/m^3
Eagle	1	12.652	0.47	0.18	49.8	15.119	0.786	112.8	11.07
Eagle	2	12.624	0.47	0.24	49.8	14.954	0.782	112.4	13.36
Eagle	3	13.894	0.50	0.27	45.3	15.178	0.808	72.0	12.90
Eagle	4	13.811	0.52	0.24	47.5	15.266	0.826	116.0	11.33
Eagle	5	13.608	0.53	0.16	47.5	15.278	0.811	76.4	12.29
Eagle	6	13.608	0.50	0.25	47.5	15.268	0.804	77.6	11.90
Upper Freeport	1	11.725	0.37	0.13	47.5	13.863	0.627	146.0	10.86
Upper Freeport	2	11.762	0.35	0.07	43.0	13.892	0.618	180.0	9.52
Upper Freeport	3	11.618	0.37	0.16	49.8	14.318	0.636	131.2	8.08
Upper Freeport	4	11.644	0.33	0.13	49.8	14.272	0.630	158.8	8.08
Upper Freeport	5	11.766	0.37	0.19	58.9	14.351	0.646	128.8	8.73
Upper Freeport	6	11.737	0.37	0.13	47.5	14.235	0.627	162.0	6.27
Blind Canyon	1	12.176	0.53	0.18	47.5	15.855	0.828	55.2	12.12
Blind Canyon	2	12.179	0.48	0.21	45.3	15.909	0.842	64.0	11.40
Blind Canyon	3	12.576	0.53	0.16	47.5	16.211	0.854	108.8	18.81
Blind Canyon	4	12.573	0.55	0.25	49.8	16.357	0.857	53.6	13.14
Blind Canyon	5	11.239	0.52	0.17	47.5	16.243	0.861	100.4	14.70
Blind Canyon	6	11.236	0.52	0.21	45.3	16.187	0.851	90.8	13.03
Wadge	1	12.651	0.53	0.12	49.8	16.510	1.108	24.0	10.12
Wadge	2	12.665	0.52	0.14	56.6	15.973	1.100	−28.8	7.37
Wadge	3	12.031	0.52	0.17	43.0	15.975	1.083	−25.2	7.26
Wadge	4	12.012	0.47	0.18	43.0	15.975	1.083	−9.2	8.28
Pittsburgh (PRL) . .	1	14.634	0.57	0.27	52.1	14.893	0.883	114.2	6.67
Pittsburgh (PRL) . .	2	14.674	0.57	0.27	47.5	15.031	0.878	139.2	4.67
Pittsburgh (PRL) . .	3	14.658	0.55	0.30	52.1	15.281	0.872	99.2	7.33
Pittsburgh (PRL) . .	4	14.675	0.53	0.32	56.6	15.094	0.871	124.8	6.00

[1]Crusher current with coal material minus the baseline crusher current without coal material (480 V).
[2]ARD level measured over a 3-min sampling period at 2 L/min.

NIOSH • Delivering on the Nation's promise: Safety and health at work for all people through research and prevention.

To receive other information about occupational safety and health problems, call
1-800-35-NIOSH (1-800-356-4674), or
visit the NIOSH Home Page on the World Wide Web at
http://www.cdc.gov/niosh

DHHS (NIOSH) Publication No. 98-160

October 1998